

4. MITSUHASHI, H., YAHATA, A., UENOTO, T., KAMATA, A., OKAJIMA, M., MURAHARA, K., and UEPPO, T.: 'p-type carrier concentration in lithium-doped zinc selenide grown by MOCVD', *J. Cryst. Growth*, 1990, 101, pp. 818-821.
5. YASUDA, T., MITSUISHI, I., and KUKIMOTO, H.: 'Metalorganic vapor phase epitaxy of low-resistivity p-type ZnSe', *Appl. Phys. Lett.*, 1988, 52, pp. 57-59.
6. STANZL, H., WOLF, K., HAHN, B., and GEDHART, W.: 'Low-pressure metalorganic vapor phase epitaxy of ZnSe-based light emitting diodes', to be published in *J. Cryst. Growth*.
7. FUJITA, S.Z., ASANO, T., MAEHARA, K., TOIYO, T., and FUJITA, S.G.: 'Photo-assisted metalorganic vapor-phase epitaxy for nitrogen doping and fabrication of blue-green light emitting devices of ZnSe-based semiconductors', *J. Cryst. Growth*, 1994, 138, pp. 737-744.
8. KUHN, W., NAUMOV, A., STANZL, H., BAUER, S., WOLF, K., WAGNER, H.P., GEDHART, W., POHL, U.W., KROST, A., RICHTER, W., DUMICHEN, U., and THIELE, K.R.: 'Low temperature MOVPE growth of ZnSe with di-tert-butylselenide', *J. Cryst. Growth*, 1992, 123, pp. 605-610.
9. FUJITA, S.Z., SAKAMOTO, T., ISEMURA, M., and FUJITA, S.G.: 'Use of methylselenol for organometallic vapor-phase epitaxy of ZnSe', *J. Cryst. Growth*, 1988, 87, pp. 581-584.
10. NISHIMURA, K., NAGANO, Y., and SAKAI, K.: 'Low temperature metalorganic vapor phase epitaxy of ZnSe and ZnSSe onto GaAs using tertiarybutylselenol', *J. Cryst. Growth*, 1993, 134, pp. 293-301.
11. RENNIE, J., ONOMURA, M., NISHIKAWA, Y., SAITO, S., PARBROOK, P.J., NITTA, K., ISHIKAWA, M., and HATAKOSHI, G.: 'High-brightness low-voltage mesa-style ZnSSe light-emitting diode', *Electron. Lett.*, 1994, 23, pp. 1090-1091.
12. EASON, D.B., HUGHES, W.C., REN, J., RIEGNER, M., YU, Z., COOK, J.W., SCHETZINA, J.F., CANTWELL, G., and HARSCH, W.C.: 'High-brightness green light-emitting diodes', *Electron. Lett.*, 1994, 30, pp. 1178-1180.

## Low polarisation dependence (< 0.3 dB) in an EA modulator using a polyimide-buried high-mesa ridge structure with an InGaAsP bulk absorption layer

K. Yamada, H. Murai, K. Nakanura, Y. Matsui and Y. Ogawa

**Indexing terms:** Electroabsorption modulators

The electroabsorption modulator combining a polyimide-buried high-mesa ridge structure with an InGaAsP bulk absorption layer which the authors have developed demonstrates an extremely low polarisation-dependent loss of less than 0.3 dB with a practical and sufficient attenuation of 20 dB.

**Introduction:** A high-speed electroabsorption (EA) modulator is a very attractive device both in multigigabit long-haul lightwave transmission systems and in optical soliton transmission systems for stabilising the generation of sech<sup>2</sup>-like optical pulse trains [1] and for in-line optical gating and optical demultiplexing [2].

Such applications, however, require that the modulator be insensitive to polarisation because optical polarisation control is very difficult in transmission lines. A modulator having a bulk material [3] has a low polarisation dependence in contrast to a modulator having a multi-quantum well (MQW) structure [4] because electroabsorption due to the Franz-Keldysh effect is inherently insensitive to light polarisation. Another important way of accomplishing this is to decrease the differential between the optical confinement factors for TE and TM polarised light. This Letter focuses on an extremely low polarisation-dependent EA modulator we have developed combining a polyimide-buried high-mesa ridge structure with an InGaAsP bulk material as the absorption layer.

**Device structure:** The EA modulator has an InGaAsP bulk absorption layer (0.26  $\mu\text{m}$  thick) with a PL peak wavelength of 1.47  $\mu\text{m}$  and an undoped InP layer (0.1  $\mu\text{m}$  thick) to prevent Zn diffusion from the upper layer (Fig. 1). All layers were grown

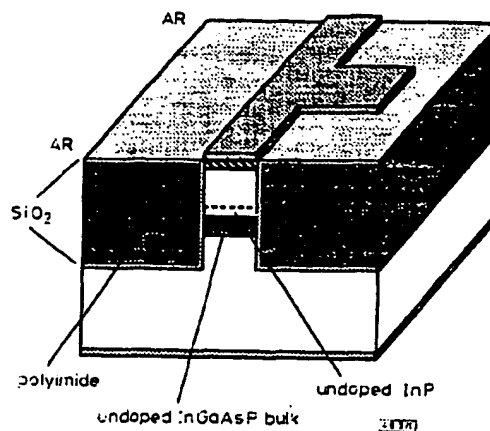


Fig. 1 Electroabsorption modulator

through single-step metalorganic vapour-phase epitaxy (MOVPE).

The high-mesa ridge structure, which is 3  $\mu\text{m}$  wide and 5  $\mu\text{m}$  deep, was formed by reactive ion etching. Both sides of the ridge waveguide were buried with polyimide to decrease the differential between the horizontal optical confinement factors of TE and TM polarised light. This structure also enables us to reduce the capacitance of the electrode pad.

The front and back facets were coated with antireflection (0.1%) film using SiO<sub>2</sub>.

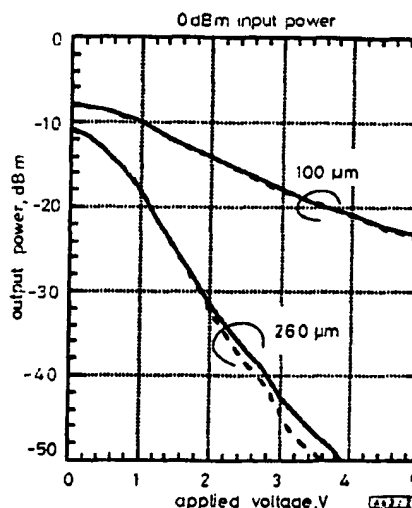


Fig. 2 Output power against reverse voltage applied ( $V_r$ ) for device lengths of 100 and 260  $\mu\text{m}$

— TE polarised light;  
--- TM polarised light

**Attenuation and polarisation dependency:** In experiments at a 1.55  $\mu\text{m}$  wavelength with an optical input power of 0 dBm for two different device lengths, 100 and 200  $\mu\text{m}$ , the extinction efficiency exceeded 10 dB/V for the 260  $\mu\text{m}$  device (Fig. 2). The insertion losses measured using tapered fibre with a curvature of 10  $\mu\text{m}$  were ~8 dB for the 100  $\mu\text{m}$  device and 11 dB for the 260  $\mu\text{m}$  device. The propagation loss was 2 dB/100  $\mu\text{m}$  and the estimated coupling loss per facet was ~3 dB, almost independent of the input light wavelength. By using aspherical lenses for optical coupling, however, we obtained an insertion loss less than 9 dB for the 260  $\mu\text{m}$  device.

The maximum polarisation dependence loss (PDL) for the 100  $\mu\text{m}$  device was 0.2 dB over the entire measured applied voltage range. For the 260  $\mu\text{m}$  device, the maximum PDL was less than 0.3 dB up to 20 dB, which represents the best data reported to date, to our knowledge, and possibly sufficient for practical application.

The PDL for a modulator with a bulk absorption layer is expressed simply as

$$PDL [dB] = 20 \log(\eta_{TM}/\eta_{TE}) + 4.343\{\Delta\Gamma L(\alpha_0 + \alpha(V))\} \quad (1)$$

where  $\eta_{TE}$  and  $\eta_{TM}$  are the coupling efficiencies per facet for TE and TM polarised light.  $\Delta\Gamma$  is the differential between the optical confinement factors for the TE and TM modes,  $L$  is the device length,  $\alpha_0$  is the absorption coefficient at a zero field, and  $\alpha(V)$  is the increase in the absorption coefficient due to the increase in the reverse applied voltage. Applying our measured PDL to the equation,  $\Delta\Gamma$  is estimated to be of the order of  $10^{-3}$ . This small  $\Delta\Gamma$  may be due to the introduction of the polyimide-buried high-mesa ridge structure and a bulk absorption layer.

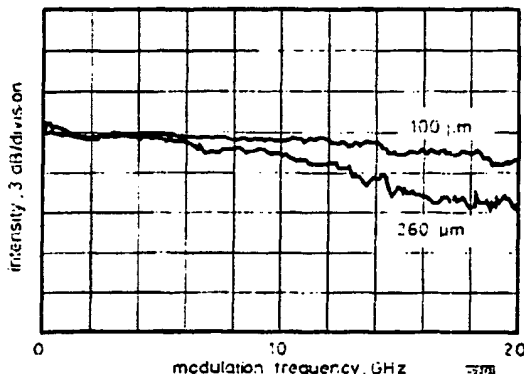


Fig. 3 Small-signal frequency responses for device lengths of 100 and 260  $\mu$ m, and  $\alpha$ -parameter against reverse applied voltage for several wavelengths of incident light for device length of 260  $\mu$ m

**High-speed, low-chirp characteristics:** The device was installed on a strip-line header with a 50  $\Omega$  terminator which was loaded parallel to the modulator, and a small-signal frequency response of 13 GHz was obtained for the 260  $\mu$ m device and >20 GHz for the 100  $\mu$ m device at a 3 dB bandwidth (Fig. 3). The value for the  $\alpha$ -parameter against reverse applied voltage is shown in Fig. 4. Values of the  $\alpha$ -parameter were estimated for several wavelengths of incident light in the 260  $\mu$ m device by using an interferometry method [5] (Fig. 4). At a reverse voltage of -1 V and 1.55  $\mu$ m wavelength, the  $\alpha$ -parameter was 0.28 and depended strongly on the reverse applied voltage. The change in the  $\alpha$ -parameter with reverse voltage, however, is smaller than that when using an MQW structure [6].

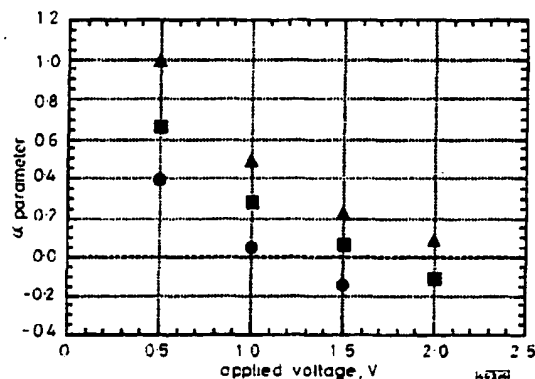


Fig. 4  $\alpha$ -parameter estimated for several wavelengths of incident light

Wavelength of incident light (nm)  
 ● 1540  
 ■ 1550  
 ▲ 1560

**Conclusion:** We have achieved an extremely low polarisation dependence in an EA modulator by combining a high-mesa ridge structure buried with polyimide and InGaAsP bulk for the absorp-

tion layer. The polarisation-dependent loss was less than 0.3 dB with an extinction ratio of 20 dB. The high-frequency bandwidth was 13 GHz and the low  $\alpha$ -parameter was 0.28, which could satisfy the practical requirements for every high-bit-rate optical transmission system.

**Acknowledgments:** We thank S. Oshiba, T. Kunii, H. Yamazaki, H. Satoh and Y. Ozeki for their invaluable advice and support.

© IEEE 1995

25 November 1994

Electronics Letters Online no: 19950115

K. Yamada, H. Murai, K. Nakamura, Y. Matsui and Y. Ogawa (Semiconductor Technology Laboratory, Oki Electric Co., Ltd., 350-5 Higashi-Sakawa, Hachioji, Tokyo 193, Japan)

## References

- SUZUKI, M., TANAKA, H., UTAKA, K., EDAGAWA, N., and MATSUSHIMA, Y.: 'Transform-limited optical pulse generation up to 20 GHz repetition rate by sinusoidally driven InGaAsP electroabsorption modulator', CLEO'92, Paper CPD-26
- SUZUKI, M., TANAKA, H., EDAGAWA, N., and MATSUSHIMA, Y.: 'New applications of a sinusoidally driven InGaAsP electroabsorption modulator to in-line optical gates with ASE noise reduction effect', *J. Lightwave Technol.*, 1992, LT-10, (12), pp. 1912-1918
- SUZUKI, M., TANAKA, H., and MATSUSHIMA, Y.: 'InGaAsP electroabsorption modulator for high-bit-rate EDFA system', *IEEE Photonics Technol. Lett.*, 1992, 4, (6), pp. 586-588
- DEVALX, F., CHELLES, S., OUGAZZADEN, A., MIRCEA, A., HUET, F., and CARRE, M.: '10 Gbit/s operation of polarization insensitive, strained InGaAsP/InGaAsP MQW electroabsorption modulator', *Electron. Lett.*, 1993, 29, (13), pp. 1201-1203
- DEVALX, F., SOREL, Y., and KERDILES, J.-P.: 'Simple measurement of fiber dispersion and chirp parameter of intensity modulated light emitter', *J. Lightwave Technol.*, 1993, LT-12, (12), pp. 1937-1940
- KATAOKA, T., MIYAMOTO, Y., HAGIMOTO, K., SATO, K., KOTAKA, L., and WAKITA, K.: '20 Gbit/s transmission experiments using an integrated MQW modulator/DFB laser module', *Electron. Lett.*, 1994, 30, (11), pp. 872-873

## Graphical analysis of contact resistance

M.G. Adlerstein

### Indexing terms: Contact resistance

Low contact resistance is a recognised advantage for high-performance semiconductor devices. This translates to requirements for semiconductor layers with low sheet resistivity and metallisations with low specific contact resistance. In the Letter we present a graphical interpretation of the importance of these requirements and illustrate the analysis for various semiconductor materials.

**Contact resistance analysis:** Low contact resistance in semiconductor devices is a recognised requirement for optimum performance. Excessive resistance increases the charging time of semiconductor layers and reduces gain. It also results in excess dissipated power at both the input and output of devices. Typically, the net resistance of a horizontal contact is a function of both the metal/semiconductor interface as well as the thickness and conductivity of the semiconductor layer beneath the metal contact.

The modelling of contact resistance has been well established in the literature, and one approach is reviewed by Shur [1]. However, one can interpret the situation with different boundary conditions and in a graphical format which gives insight into the contributing factors. Horizontal contacts are modelled as shown schematically in Fig. 1. The resistor network models the distributed current flow in the structure. The metal contact resistance is represented by a network of parallel resistors (each with a value  $R_p$ ) feeding a string of series resistors (each with a value  $R_s$ ) which model the horizontal flow through the semiconductor layer. A network where the density of resistors tends toward infinity represents continuous material layers. The value of the resistors can be defined in terms

respectively. These losses are relatively low compared to those of Si IID waveguides ( $\sim 40\text{dB cm}^{-1}$ ) [3]. In contrast, a loss of about  $50\text{cm}^{-1}$  ( $\sim 210\text{dB cm}^{-1}$ ) has been calculated in the untreated lasers with  $500\text{ }\mu\text{m}$  long passive waveguides.

**Conclusion:** Oxide stripe bandgap shifted lasers have been fabricated from the material intermixed to different degrees using a novel plasma intermixing technique. Results indicate that the material is still of high quality after intermixing.

Oxide stripe extended cavity lasers have been fabricated to demonstrate the use of the plasma technique in a photonic integrated circuit application. The results show that selective quantum-well intermixing helped to reduce the threshold current by a factor of 5. Losses as low as  $18\text{dB cm}^{-1}$  have been measured in a laser with a  $500\text{ }\mu\text{m}$ -long extended cavity section intermixed using the plasma damage induced layer intermixing process.

**Acknowledgments:** The authors would like to thank J.S. Roberts of Sheffield University for growing the MOVPE wafer used in this study. This work was supported by the Engineering and Physical Sciences Research Council (UK) under grant GR/H/82471.

© IEE 1995

1 February 1995

Electronics Letters Online No: 19950342

B.S. Ooi, A.C. Bryce and J.H. Marsh (Department of Electronics and Electrical Engineering, University of Glasgow, Glasgow G12 8QQ, United Kingdom)

#### References

1. OOI, B.S., BRYCE, A.C., WILKINSON, C.D.W., and MARSH, J.H.: 'Study of reactive ion etching-induced damage in GaAs/AlGaAs structures using a quantum well intermixing probe', *Appl. Phys. Lett.*, 1994, 64, p. 598
2. ANDREW, S.R., MARSH, J.H., HOLLIAND, M.C., and KEAM, A.M.: 'Quantum well laser with integrated passive waveguide fabricated by neutral impurity disordering', *IEEE Photonics Technol. Lett.*, 1992, 4, p. 426
3. WERNER, J., LEE, T.P., KAPON, E., COLAS, B., STOFFEL, N.G., SCHWARZ, S.A., SCHWARTZ, L.C., and ANDREADAKIS, N.C.: 'Single and double quantum well lasers with a monolithically integrated passive section', *Appl. Phys. Lett.*, 1990, 57, p. 810

## Highly efficient optical phase modulator in SOI waveguides

C.K. Tang and G.T. Reed

**Indexing terms:** Silicon-on-insulator, Optical waveguides, Phase modulation, Optical modulation

The realisation of a low-loss, highly efficient, singlemode optical phase modulator in SOI is reported. At a wavelength of  $1.5\text{ }\mu\text{m}$  the figure of merit for the device, the induced phase shift per volt per millimetre, is greater than  $200^\circ\text{V/mm}$ . To our knowledge, this is the highest reported value to date. In addition, the device drive current ( $< 10\text{mA}$ ) is thought to be the lowest yet reported.

**Introduction:** Silicon is the backbone of the microelectronics industry, and its initial role in integrated optics as a substrate material is now changing to that of the guiding medium itself. Today silicon-based waveguides exhibit losses of well below  $1\text{ dB/cm}$  (see, for example [1, 2]). Silicon technology is well established and relatively inexpensive. The potential of silicon electronic circuits integrated monolithically with silicon guided-wave devices has generated much interest in developing low-cost silicon-based integrated optical devices.

Optical waveguides, bends,  $\pi$ -junctions [3], optical switches and modulators [4–7] in silicon have received much attention in recent years. In this Letter we describe the characteristics of an optical phase modulator fabricated in SIMOX material (separation by implantation of oxygen).

Electric fields, free carriers and the thermo-optic effect provide potential mechanisms for modulation of the refractive index (and therefore phase) in silicon. In 1987 Soref and Bennett studied the refractive index change in silicon [8] due to the Franz-Keldysh effect, the Kerr effect and charge carrier effect. They concluded that for experimentally reasonable values of applied field and injected carriers the changes in refractive index were at least two orders of magnitude larger for the latter.

Integrated electro-optic switches in silicon reported to date have been based on rib waveguides in epitaxial silicon [6] and SOI waveguides [7]. The former have suffered from relatively high waveguide losses, and many of both types have required relatively high current densities as well as high switching currents [6] of the order of  $1 \times 10^4\text{ A/cm}^2$  and (200–300 mA), respectively. This has led to the thermo-optic effect (TOE) [9] competing with the free-carrier effect to change refractive index in opposing senses, and consequently has resulted in inefficient devices. Singlemode TOE switches/modulators have also been realised [9], although the high power requirements ( $\sim 245\text{mW}$ ) may limit the practical use of such devices.

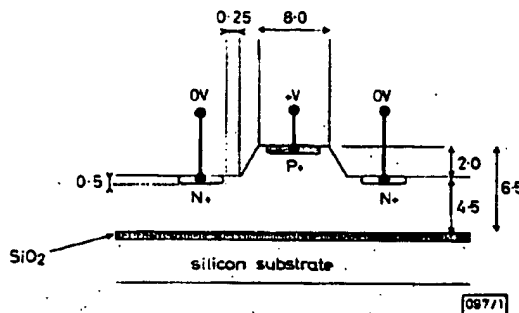


Fig. 1 Cross-section through active region of device

All dimensions in  $\mu\text{m}$

In this Letter we describe the characteristics of an elongated *pin* diode embedded in a singlemode optical waveguide. Fig. 1 shows the cross-section through the active region of the device. The operating principle of the modulator is as follows: application of a forward bias injects carriers into the central waveguiding area, thus altering the local refractive index and therefore the phase of a propagating optical wave. MEDICI, a two-dimensional semiconductor simulation program, was employed to optimise the overlap of the injected carrier profile and the fundamental optical mode profile and therefore the phase change of the optical wave for a given applied voltage [10]. This was achieved by optimising the device geometry.

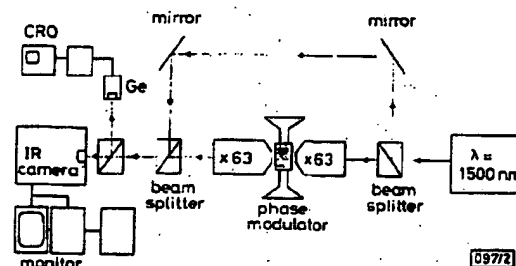


Fig. 2 Schematic diagram of Mach-Zehnder interferometer used to measure phase change

The modulator was incorporated into one arm of a free-space Mach-Zehnder (M-Z) interferometer as shown in Fig. 2. Light passing in one arm of the interferometer may be subjected to a phase shift if the necessary voltage is applied to the *pin* diode modulator on that arm of the Mach-Zehnder interferometer. The interference between the two arms produces a series of fringes at the output arm of the M-Z. We can determine the required voltage  $V_\pi$  to produce a  $\pi$  phase shift by observing the phase shift in the fringes as the applied voltage is increased. Modulation of the

output is thus achieved by a voltage-controlled phase shift in one arm of the M-Z interferometer.

**Results:** KOH etching along the (1,1,1) plane was used to produce smooth sidewalls and therefore low scattering losses. The measurement losses of the realised waveguide were lower than 1 dB/cm. The device had the dimensions shown in Fig. 1 and had an interaction length of 500  $\mu$ m, and the waveguides were singlemode and had multi-micrometre dimensions, supporting the work of Soref *et al.* [11].

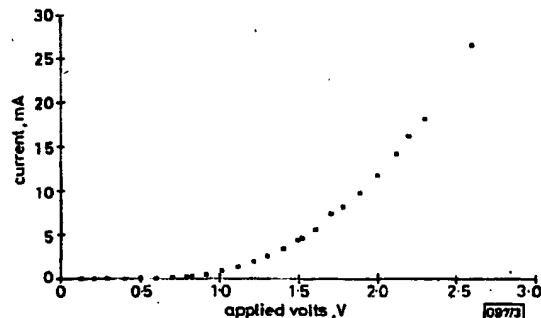


Fig. 3 Forward characteristic of silicon pin diode modulator

The forward characteristics of the device are shown in Fig. 3. The electrical characteristic is, as expected, that of a silicon diode.

Observation of a  $\pi$  phase shift in the fringes occurred for an applied forward bias of  $V_f = 1.7$  V. The current flowing through the phase modulator at this applied voltage was recorded as  $I_{mod} = 7$  mA.

A figure of merit  $\eta$  can be defined as the induced phase shift per volt per mm,

$$\eta = \pi / V_n L_n = 212^\circ / \text{V/mm}$$

where  $L_n$  is the interaction length of the modulator for a  $\pi$  phase shift in millimetres ( $\approx 0.5$  mm).

Assuming that the current flows through the rib, we can approximate the junction area as  $A = wL$ , and so current density  $J = 175 \text{ A/cm}^2$ , where  $w$  is the waveguide width and  $L = L_n$ .

The current density of the device is approximately an order of magnitude lower when compared to previously reported devices in silicon [6, 7]. A limitation of the modulators in silicon to date has been the relatively large power requirement which has led to the TOE playing a very significant role [4]. Taking a 1-dimensional simplified treatment of heat transfer and assuming negligible heat losses from convection and radiation losses and no lateral diffusion of heat energy, we can approximate the heat transport from the heater to the silicon as

$$P = VI = \Delta T w L / (t_{si} / k_{si}) = 11.9 \text{ mW}$$

where  $t_{si}$  is the thickness of the silicon layer and  $k_{si}$  is the thermal conductivity of silicon. We find  $\Delta T = 0.138 \text{ K}$ . Because silicon exhibits a refractive index change due to temperature,  $\Delta n_{temp}$ , of  $1.86 \times 10^{-5} \text{ K}^{-1}$ , the ratio of the refractive index change due to free carrier effect and that due to the thermo-optic effect can be expressed as  $\Delta n_{nc} / \Delta n_{temp} = 58$ . So for this device the thermo-optic effect is negligible.

**Conclusion:** We have realised a highly efficient, singlemode, low-loss, multi-micrometre silicon pin-diode modulator, which has very low operating power requirements. The thermo-optic effect has been shown to be negligible.

**Acknowledgments:** The authors are grateful to TMA for provision of the MEDICI software, to Southampton University for assistance with device fabrication, and the first author is grateful to EPSRC and Bookham Technology Ltd for financial support.

© IEE 1995  
Electronics Letters Online No: 19950328

30 January 1995

C.K. Tang and G.T. Reed (Department of Electronic and Electrical Engineering, University of Surrey, Guildford, Surrey, GU2 5HX, United Kingdom)

## References

- 1 RICKMAN, A., REED, G.T., WEISS, B.L., and NAMAVAR, F.: 'Low loss planar optical waveguides fabricated in SIMOX material', *IEEE Photonics Technol. Lett.*, 1992, 4, pp. 633-635
- 2 SCHMIDTCHEN, J., SPLETT, A., SCHUPPERT, B., PETERMANN, K., and BURBACH, G.: 'Low-loss singlemode optical waveguides with large cross-section in silicon-on-insulator', *Electron. Lett.*, 1991, 27, pp. 1486-1488
- 3 RICKMAN, A., and REED, G.T.: 'Silicon on insulator optical rib waveguides: Loss, mode characteristics, bends and Y-junctions', *IEEE Proc. Optoelectron.*, 1994, 141, pp. 391-393
- 4 FISCHER, U., SCHUPPERT, B., and PETERMANN, K.: 'Integrated optical switches in silicon based on SiGe-waveguides', *IEEE Photonics Technol. Lett.*, 1993, 5, (7), pp. 785-787
- 5 TREYZ, G.V., MAY, P.O., and HALBOUT, J.-M.: 'Silicon Mach-Zehnder waveguide - interferometers based on the plasma dispersion effect', *Appl. Phys. Lett.*, 1991, 59, (7), pp. 771-773
- 6 LORENZO, J.P., and SOREF, R.A.: '1.3  $\mu$ m electro-optic silicon switch', *Appl. Phys. Lett.*, 1987, 51, (1), pp. 6-8
- 7 XIAO, X., STURM, J.C., GOEL, K.K., and SCHWARTZ, P.V.: 'Fabry Perot optical intensity modulator at 1.3  $\mu$ m in silicon', *IEEE Photonics Technol. Lett.*, 1991, 3, (3), pp. 230-231
- 8 SOREF, R.A., and BENNETT, B.L.: 'Electro-optical effects in silicon', *IEEE J. Quantum Electron.*, 1987, QE-23, pp. 123-129
- 9 MAYER, R.A., JUNG, K.H., LEE, W.D., KWONG, D.-L., and CAMPBELL, J.C.: 'Thin film thermo-optic GeSi Mach-Zehnder interferometer', *Opt. Lett.*, 1992, 17, (24), pp. 1812-1814
- 10 TANG, C.K., REED, G.T., WALTON, A.J., and RICKMAN, A.G.: 'Low loss, single-mode, optical phase modulator in SIMOX material', *IEEE J. Lightwave Technol.*, 1994, 12, (8), pp. 1394-1400
- 11 SOREF, R.A., SCHMIDTCHEN, J., and PETERMANN, K.: 'Large single-mode rib waveguide in GeSi-Si and Si-on SiO<sub>2</sub>', *IEEE J. Quantum Electron.*, 1991, 27, pp. 1971-1974

## InGaAsP/InP strained MQW laser with integrated mode size converter using the shadow masked growth technique

I. Moerman, M. D'Hondt, W. Vanderbauwhede, P. Van Daele, P. Demeester and W. Hunziker

**Indexing terms:** Integrated optics, Optical couplers, Semiconductor junction lasers, Semiconductor quantum wells

The authors report the realisation of a planar buried-heterostructure (PBH) strained multiquantum-well (MQW) laser emitting at 1.52  $\mu$ m with integrated vertical taper using the shadow masked growth (SMG) technique. The threshold current is 8 mA and the coupling loss to a cleaved singlemode fibre is only 3.3 dB.

**Introduction:** In optical communication systems several optical interconnections between semiconductor optoelectronic devices and singlemode fibres are required. The very small refractive index difference in a glass fibre results in a weakly guided optical mode with a typical mode size of 8 - 10  $\mu$ m for 1.55  $\mu$ m wavelength. Because the mode size in an optoelectronic waveguide device is much smaller ( $< 2 \mu$ m) and generally highly asymmetric, there is large mode mismatch between the fibre mode and the device mode, and therefore the fibre-chip coupling efficiency is low.

During the past few years, many researchers have focused on the integration of mode size converters with optoelectronic waveguide components, to achieve a larger and more symmetric near-field pattern at the device facet ([1] and references therein). Such components allow low coupling losses and large alignment tolerances and hence lower packaging costs.

We have previously demonstrated the monolithic integration of a mode size converter with a PBH InGaAsP/InP double-heterostructure laser using the SMG technique, which exhibited a coupling loss as low as 4.8 dB to a cleaved singlemode fibre [2]. In this Letter we present a PBH InGaAsP/InP strained MQW laser with integrated mode size transformer and a coupling loss of 3.3 dB.

BEST AVAILABLE COPY